Walking and Running with Passive Compliance:
Lessons from Engineering a Live Demonstration of the ATRIAS Biped

Christian Hubicki†, Andy Abate†, Patrick Clary†, Siavash Rezazadeh, Mikhail Jones, Andrew Peekema, Johnathan Van Why, Ryan Domres, Albert Wu, William Martin, Hartmut Geyer, and Jonathan Hurst

***Abstract*—Biological bipeds have long been thought to take advantage of compliance and passive dynamics to walk and run, but realizing robotic locomotion in this fashion has been difficult in practice. ATRIAS is a bipedal robot designed to take advantage of inherent stabilizing effects that emerge as a result of tuned mechanical compliance. We describe the mechanics of the biped and how our controller exploits the interplay between passive dynamics and actuation to achieve robust locomotion. We outline our development process for incremental design and testing of our controllers through rapid iteration. By show time at the DARPA Robotics Challenge, ATRIAS was able to walk with robustness to large human kicks, locomote in terrain from asphalt to grass to artificial turf, and traverse changes in surface height as large as 15 cm without planning or visual feedback. Further, ATRIAS can accelerate from rest, transition smoothly to an airborne running gait, and reach a top speed of 2.5 m/s (9 kph). This endeavor culminated in seven live shows of ATRIAS walking and running, with disturbances and without falling, in front of a live audience at the DARPA Robotics Challenge. We conclude by enumerating what we believe were the key lessons learned in the process of developing these capabilities.**

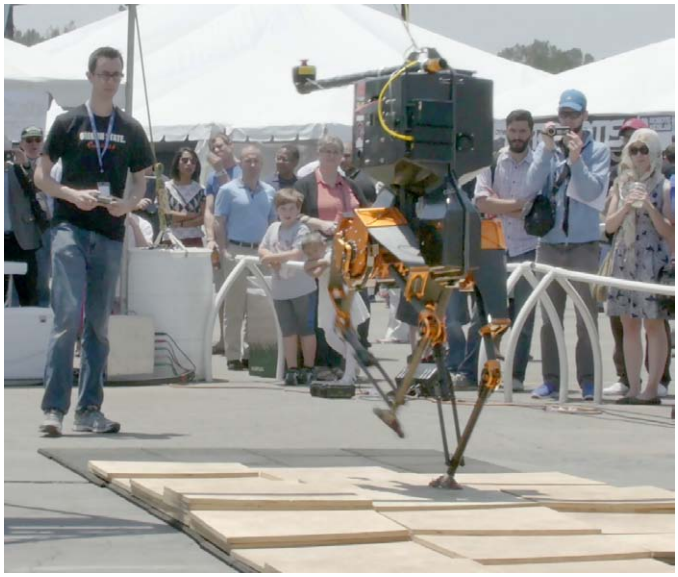

Fig. 1. The ATRIAS bipedal robot performing one its seven live dynamic demonstrations in front of a live audience at the DARPA Robotics Challenge. As one component of the show, the spring-legged robot is commanded to walk over uneven surfaces without visual sensing or external support. Reliably achieving such dynamic locomotion in an uncertain environment required rigorous development and testing of the hardware, software, and control algorithms. Here, we describe the purpose of this demonstration and how we approached engineering fast and robust robotic walking and running that can be performed reliably under the scrutinizing public eye.

I. Introduction

Walking and running on two legs is an enduring challenge in robotics. Avoiding falls becomes especially tricky when the terrain is uncertain in both its geometry and rigidity. A promising approach to achieve stable control is to relinquish some authority to purposeful passive dynamics, perhaps by adding mechanical compliance (Raibert, 1986) or removing actuators entirely (McGeer, 1990). If the machine's unactuated dynamics are thoughtfully designed, they can passively attenuate disturbances and require smaller adjustments from the controller (Pfeifer et al., 2006).

The ATRIAS biped (Hubicki et al., 2015) is a physical embodiment of this mechanical intelligence approach (Blickhan et al., 2007), equipped with four degrees of passive compliance in its legs and motor-free pin joints for feet. While eschewing actuators and inserting springs makes control less formally tractable (Spong, 1998), we found that thoughtfully applying insights from reduced-order models (Rezazadeh et al., 2015) can yield a range of agile and stable locomotion behaviors. In doing so, we aim to demonstrate that 3D bipedal walking and running is not only possible with a passive-dynamics based approach, but the result is sufficiently robust that it can serve as a viable framework for practical locomotion in unstructured environments. To make our case, we resolved to test ATRIAS' locomotion mettle in front of a live audience at the DARPA Robotics Challenge Expo (snapshot of a performance shown in Figure 1).

Zero Moment Point (ZMP) approaches have long been the go-to methods for generating stable bipedal locomotion (Vukobratovic and Borovac, 2004). The core strategy of maintaining full actuation though flat-footed contact is at the heart of the field's most visible humanoids, including ASIMO, HUBO, and the HRP-series humanoids (Sakagami et al., 2002; Park et al., 2006; Kaneko et al., 2009). Given its track-record of success, elaborations of this basic ZMP concept (Kajita et al., 2003) were ubiquitous at the high-stakes DARPA Robotics Challenge (Zucker et al., 2015; Feng et al., 2015; Johnson et al., 2015; Kohlbrecher et al., 2015; Yi et al., 2015; Kuindersma et al., 2015). However, these approaches require planning with respect to the environment in order to ensure ZMP criteria. As terrain becomes less structured and locomotion becomes faster, such planning becomes more difficult to rely upon for locomotion stability.

In contrast to a planning approach, locomotion has

† The primary authors contributed equally to this work.

also been studied as a potentially "self-stable" phenomena (Seyfarth et al., 2003). Using reduced-order "spring-mass" models (Blickhan, 1989), locomotion strategies have been developed to mitigate (Schmitt and Clark, 2009) or entirely reject disturbances without feedback (Ernst et al., 2012). These passively compliant models and corresponding simple control strategies have been theoretically extended across walking and running (Geyer et al., 2006; Vejdani et al., 2015). These math models, while simple, are sufficiently relevant to biological locomotion that they are commonly used to analyze stabilization in animal locomotion (Full and Koditschek, 1999; Jindrich and Full, 2002; Moritz and Farley, 2004; Daley and Biewener, 2006). Like animals, our robot will not precisely match these simple math models, but we too may use insights and general behaviors of spring-mass systems to guide the control policies of our robot toward self-stability.

Likely the most famous examples of insight-driven biped control were the Raibert hoppers (Raibert, 1986) and its successors (Ahmadi and Buehler, 2006), which were amazingly agile, but required power through an off-board pneumatic tether. Other examples include the hyper-efficient walkers (Collins et al., 2005; Bhounsule et al., 2014), which also had control designed to work effectively with their passive dynamics. Recognizing some merit to passive dynamics and compliance, formal approaches have begun rising to the challenge of underactuation in robotics (Spong, 1994; Manchester et al., 2011). Variations on methods such as hybrid zero dynamics (Westervelt et al., 2003) have been successful in achieving planar walking, both with (Sreenath et al., 2011; Park et al., 2012; Hereid et al., 2014) and without compliance (Martin et al., 2014), as well as running (Sreenath et al., 2013) and preliminary walking implementation in 3D (Buss et al., 2014). Other methods have begun to show promise in simulation for achieving robust bipedal running (Erez et al., 2013; Wensing and Orin, 2013).

Our specific goal at the DARPA Robotics Challenge (DRC) was to exhibit robust walking and running over unstructured terrain with all components, including batteries, onboard the machine. The purpose is to demonstrate the practical potential of this compliant approach to bipedal locomotion. With these soft spring-leg mechanisms, we were able both to walk and smoothly accelerate up to running speeds (2.5 m/s). The dynamic approach to stability allowed ATRIAS to recover from large unmodeled impulses (i.e. kicks). Further, we demonstrated walking over uneven ground without any vision or preparative planning, including 15-cm steps and nonrigid terrain. The resulting locomotion is also efficient compared to bipeds of similar scale, with a total cost of transport of 1.3 (ASIMO is estimated to have a total transport cost of 3.2 (Collins and Ruina, 2005)).

Here we describe the overall approach to engineering ATRIAS, an overview of how we control it, and our incremental approach to testing it for live demonstrations. In Section II, we describe the philosophy and mechanics of the robot's construction, and we detail the electronics/software infrastructure. In Section II-C, we provide an overview of the control algorithms used to control ATRIAS, which are designed specifically for the compliant dynamics of the machine. Section III describes our testing and development process, taking ATRIAS from simple stepping in 2D through robust and fast 3D locomotion. Finally, in Section V-VI-B we summarize ATRIAS' capabilities, the performance at the DRC event, and lessons learned from the process of developing this live demonstration.

ATRIAS at a Glance

Top speed	2.5 m/s
Max ground height variation	15 cm
Max kick impulse	60 kg·m/s
Surface incline	15 deg
Aerial phase during running	30 ms
Mechanical Cost of Transport	1.0
Total Cost of Transport	1.3
Battery life	30 minutes
Leg length	1.0 m
Height	1.7 m
Weight	60 kg
Spring stiffness	3 kN·m/rad
Leg stiffness @ 0.9 m rest length	20 kN/m
Control Rate	1.0 kHz
Lines of controller code	880

II. Robot Overview

ATRIAS is designed to perform highly dynamic walking and running gaits. Complementary passive hardware, a mechanism which is just as dynamic as the locomotion itself, allows the biped to be reactive and stable when disturbed. Because the hardware and algorithms are equal partners in generating the locomotion patterns, the method used to control ATRIAS would not function without the intended natural dynamics built into the mechanisms[1].

A. Mechanical Overview

Even with pantograph legs unlike anything seen in nature, ATRIAS performs bouncy gaits and reacts to trips and falls in a convincingly natural way. Its construction is a result of an effort to reproduce the *natural dynamics* and passive responses found in nature, rather than mimic any particular morphology (Hubicki et al., 2015). Figure 2 shows the full biped robot, highlighting important components and providing references to product part numbers.

Many animals, including humans, have walking and running gaits that can be described by springy, mathematically simple legs. A common spring-mass model is the Spring-Loaded Inverted Pendulum (SLIP) model, with a point-mass body, a massless point toe, and a massless linear spring connecting the two. When in contact with the ground, the toe is assumed to be in perfect contact and completely fixed. When leg forces drop to zero, the toe is no longer fixed to the ground and moves rigidly with the point mass. This model is completely

[1] Alternatively, sufficiently high-bandwidth actuation and high control rates could simulate these natural dynamics, but simulating these dynamics typically requires higher-powered or very torque-dense actuators (Boaventura et al., 2012; Park et al., 2015).

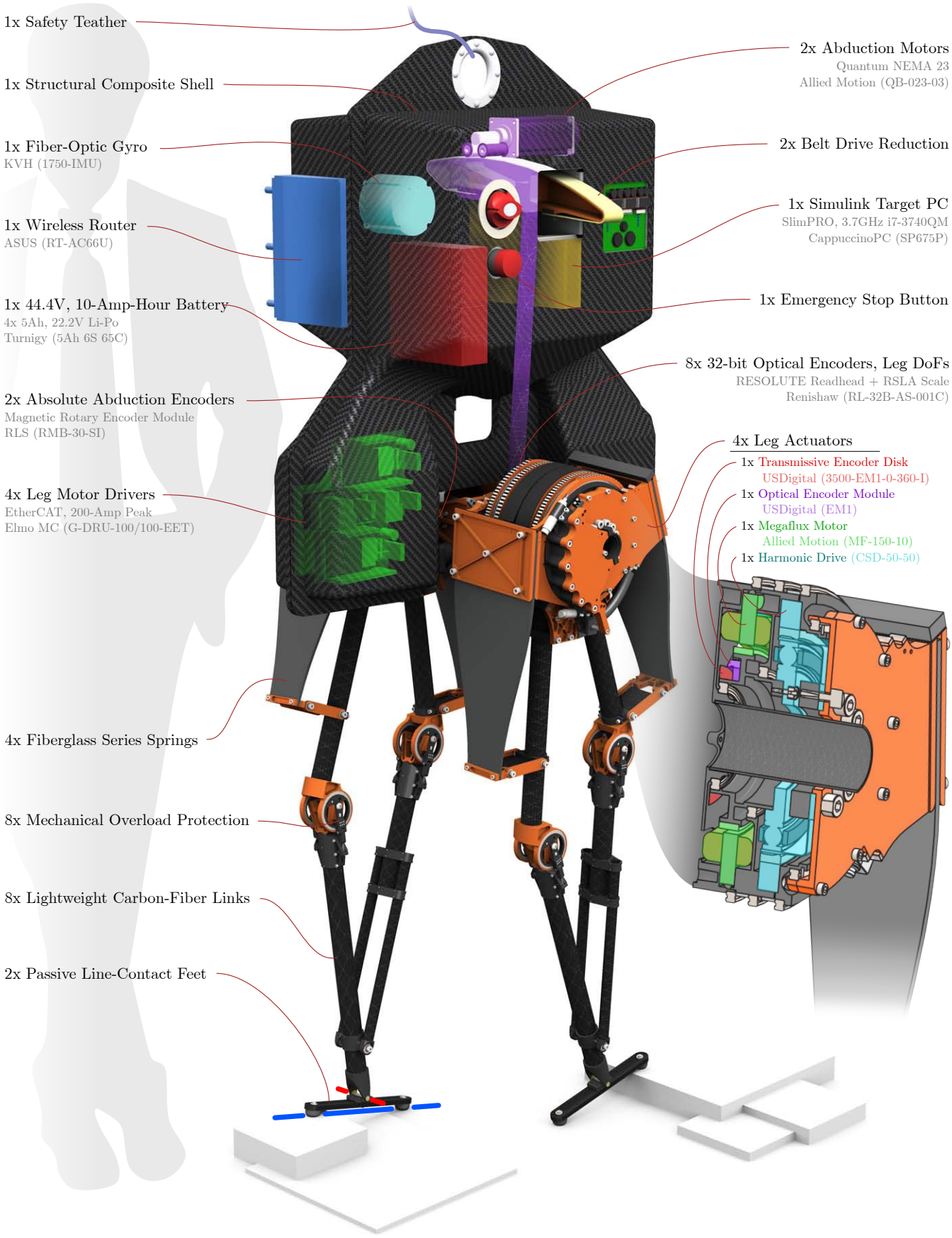

Fig. 2. Rendered view of ATRIAS with mechanisms and features highlighted. Most systems are located in the composite torso, with only actuation and sensing on the legs. Part numbers and suppliers are provided for selected components.

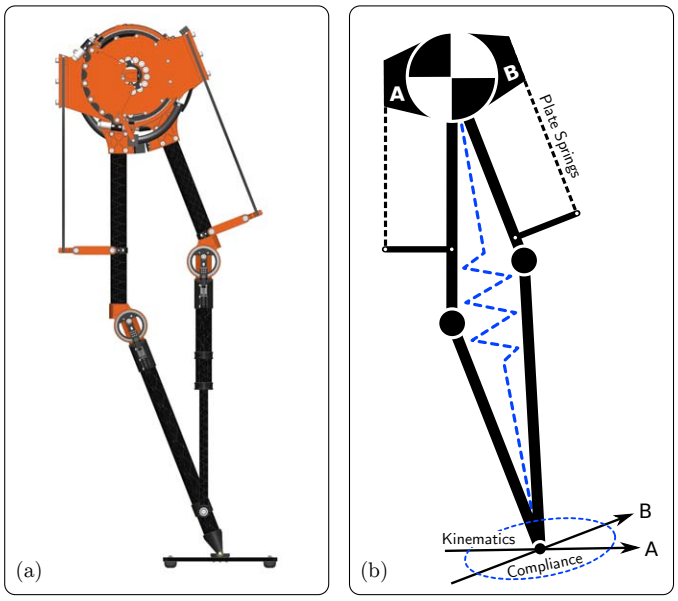

Fig. 3. (a) Rendered view of the ATRIAS leg design. (b) Schematic view showing kinematics and compliant behavior of the toe. Two motors co-located at the hip drive each input link of a parallel mechanism. Plate springs connect the links to the motors, providing series compliance and smoothing input forces. All heavy components are located at the hip, and the parallel mechanism is composed of lightweight carbon-fiber links. This morphology has dynamics matching the Spring-Loaded Inverted Pendulum (SLIP) template (Schwind, 1998). Motor A and B basis vectors are drawn at the toe to illustrate the kinematics of this pose. The instantaneous motion of the toe is the weighted sum of these basis vectors. Similarly, a compliance ellipse shows the elastic behavior of the physical toe around the neutral point (Abate et al., 2015); the ellipse represents the deflection of the toe for a unit force in all directions, so the major axis is soft and the minor axis is stiff.

energy conservative, because the toe is massless, and there is a massless spring between the toe contact and the point mass; it can walk or run continuously as long as the average ground height is consistent.

Observers can see the influence of spring-mass models in the ATRIAS design: carbon-fiber legs for minimum inertia connected by series springs to the concentrated mass at the hips. Such construction gives the biped noticeably SLIP-like dynamics (Figure 3). With series compliance, unforeseen impacts are softened, and energy can be recycled from step to step, energy can be released at higher rates than the motor alone can deliver. These combined factors have the potential to improve robustness of the mechanism as well as energetic efficiency.

Kinematically, ATRIAS has two planar legs comprising a parallel mechanism, two actuators co-located at the hip, and a distal toe. Each leg has an abduction degree of freedom, which both share an axis in the sagittal plane of the torso. Six total actuators exist on the robot[2]: two legs, each with hip extension, knee extension and hip abduction. The robot lacks long-axis rotation of the hip, and thus cannot actively turn.

A passive foot is attached at the ankle in a way which simulates a point contact at the ground, but restricts yaw rotation, thereby removing this degree of freedom from the dynamics of the robot. The two-point line contacts at the bottom of the feet keep ATRIAS pointed in roughly the same direction between steps, resisting inertial forces from the heavily under-actuated robot (Abate, 2014).

Mechanical fuses at the knees protect the robot from damage due to excessive sideloads at the toe. This resistance to significant damage makes rapid iteration and testing possible. Expensive and difficult repairs to bearings, the transmission, and the carbon-fiber leg would halt progress, but fuses are easy to reattach.

Because ATRIAS is a prototype experimental platform, it is fairly fragile and cannot withstand torso collisions or falls. A portable gantry system protects the robot from falls via a safety line. During operation, the line is kept slack as to not affect the robot's dynamics unless it drops or goes wildly off course. ATRIAS is otherwise entirely self-contained, and this connection is only meant to catch the robot in the event of a malfunction.

B. Electrical/Software Overview

ATRIAS' electrical architecture is built around commodity PC hardware, custom sensor interface boards, and off-the-shelf motor drivers. An EtherCAT data bus provides high-throughput, real-time communication between the system components and interfaces directly with the Simulink real-time operating system. Commercial off-the-shelf (COTS) lithium polymer batteries power the motor drivers as well as the computer and other components through COTS DC-DC voltage regulation modules. Figure 4 shows the major components of the electrical system.

All control processing is done with an onboard, miniature desktop computer. This computer is a commercially-available small-form-factor PC based on a modern Intel desktop processor. The robot computer executes our control software, developed in MATLAB and Simulink, on top of the Simulink Real-Time kernel. The Simulink kernel ships with drivers for using the EtherCAT protocol with standard Ethernet chipsets, which is used to retrieve sensor data and send torque commands to the motor drivers.

ATRIAS' six motors are driven with two different types of motor amplifier. The hip extension and knee extension motors use EtherCAT-enabled COTS servo drivers, capable of supplying a peak current of 200 Amps. The hip abduction motors are driven by smaller COTS motor drivers capable of a peak current of 60 Amps. All of these drive three phase brushless motors in current control mode, using Hall effect sensors and an incremental encoder for sinusoidal commutation.

ATRIAS uses only proprioceptive sensing for control, and is otherwise blind to the environment. High-resolution absolute encoders at each internal degree of freedom provide joint angles and spring deflections, and a fiber optic gyroscope provides torso orientation. These sensors are sufficient to determine the configuration of the robot save for its translation with respect to the the world frame.

Custom, versatile interface modules (called "Medulla" modules) read, translate, packetize and send proprioceptive

[2]Note that ATRIAS has 13 degrees of freedom, and thus is heavily underactuated for a bipedal robot.

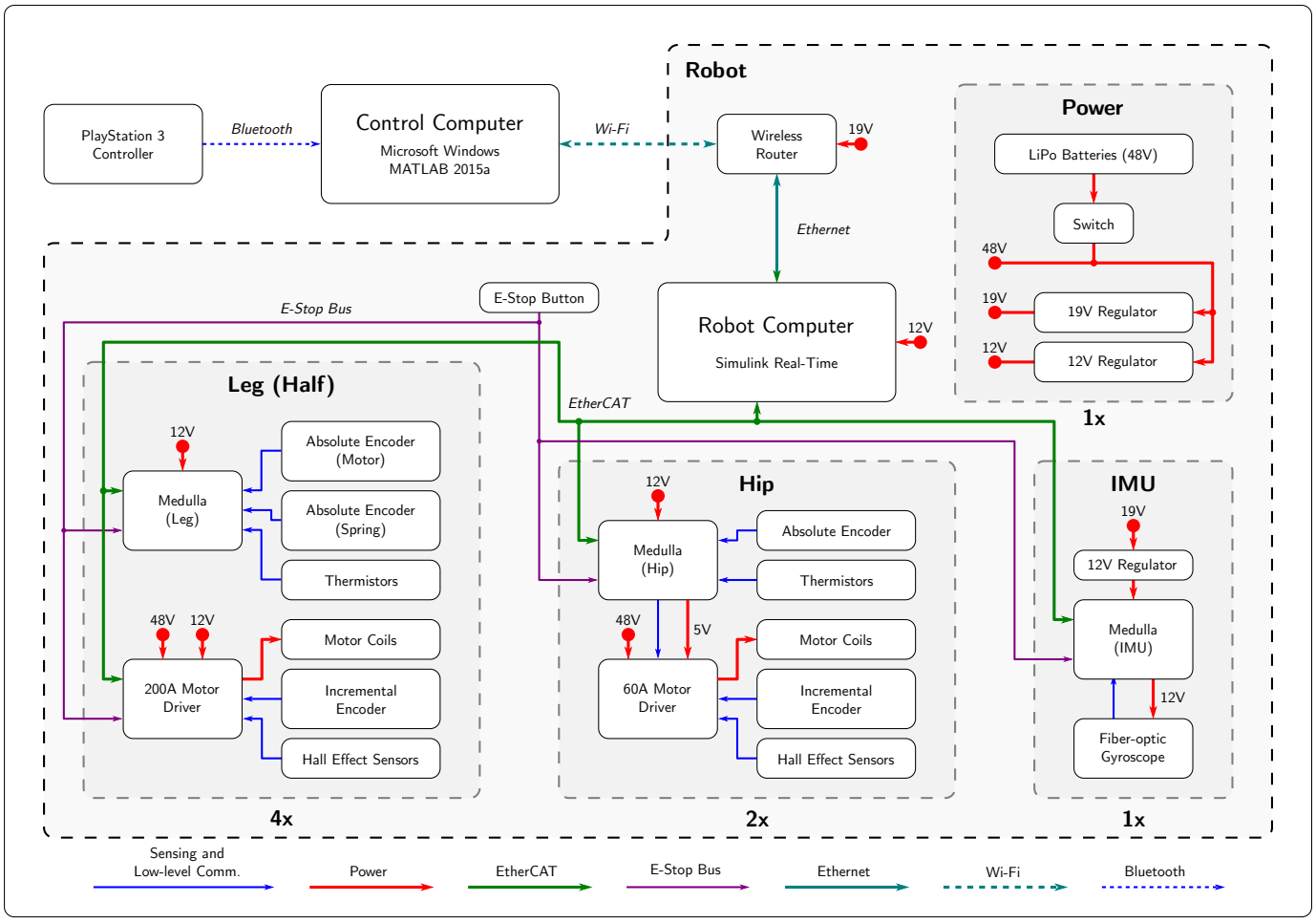

Fig. 4. Connection diagram of the electrical system. Control commands are sent by the human operator using a PlayStation 3 controller, which are then sent over WiFi to a router on the robot. Motor power is provided by Li-Po batteries, and regulated down to two logic levels to supply supporting systems. EtherCAT is the primary means of communication between systems, connecting the compiled Simulink realtime operating system to the EtherCAT-enabled motor drivers and the custom Medulla microcontrollers. The Medullas are used for collecting low-level sensor data to broadcast over EtherCAT. An emergency stop system disables all motor drivers, which can be triggered either by software or by a physical button located on the robot.

and orientation sensor data to the control computer. The Medullas also read thermistors embedded in the motor assemblies so that the controller can detect and respond to overheating. Some Medulla modules are used to pass torque commands to the hip abduction motor drivers, as these motor drivers cannot connect directly to the EtherCAT bus.

The battery pack uses four, six-cell lithium polymer battery packs, each with a 5 Amp-hour rated capacity. The packs are connected in a two-serial two-parallel configuration, giving a nominal voltage of 44.4 Volts and a nominal capacity of 10 Amp-hours. With 65C-discharge-rate batteries, the pack is rated to deliver a peak current of 650 Amps.

A supervisory computer communicates with the robot computer over a WiFi link, through a wireless router mounted on the robot. The supervisory computer, a laptop running MATLAB and Simulink on Windows 8.1, displays diagnostic information and is used to calibrate and enable the robot. Movement commands are generated by a PlayStation 3 controller connected to the supervisory computer, then sent over the wireless link to the robot computer.

The robot uses an emergency stop (E-Stop) system to disable the motor drivers and prevent damage to the robot or injury to operators. An "E-stop" bus with ring topology allows stop signals or physical breaks in the bus to reliably propagate to everything in the chain. When the bus is pulled high, the motor drivers are enabled and allowed to send current to the motors. When the pull-up is removed — either due to a "stop" condition generated by the robot computer, the emergency stop button being pressed, or a wire being severed — current to the motors is disabled and the Medulla modules enter a "stop" state.

C. Control Algorithm Overview

Controllers used on ATRIAS are designed to work with the dynamic hardware. We use reduced-order and mechanical insights to develop behaviors rather than high-DOF model-based control. The behaviors do not require any preplanning, and the stability of the gait is not tied to the existence of disturbance models. Instead, the robot is purely reactive to the changing world.

Joint compliance relates forces to deflections, measurable with the high-accuracy joint encoders and allowing open-loop

trajectories to interact with unexpected or non-trivial contact states. Knowing that forces will be exerted exactly opposite to contact disturbances, we can create controllers which are open-loop stable with respect to changes in the environment. In a similar way to hardware compliance, low gains for motor trajectory tracking allow the controller to loosely track discontinuous trajectories without inducing extreme accelerations.

Several simultaneous behaviors create the overall behavior of the robot. Controllers blend together based on leg force rather than switching out distinct controllers for different phases of the gait. Figures 5-8 illustrate the concepts used in the control algorithm: (1) clock-based stepping, (2) velocity-based foot placement, (3) soft transitions between swing and stance, (4) torso balance, and (5) energy injection against controlled damping. These behaviors are in effect for both legs simultaneously, and the individual progressions are phase-shifted by the alternating clocks for each leg. A detailed look at the controller can be found in Rezazadeh et al. (2015).

1) Clock-Based Stepping: Stepping is based on a clock cycle, where the frequency of steps matches the natural frequency of the spring-mass dynamics of the robot. In effect, the system as a whole acts similarly to a forced oscillator with dissipation, which entrains the robot to a dynamic oscillating gait (Figure 5b). Stepping trajectories are parameterized by a stepping height (the apex of the step trajectory) and a nominal touchdown target which is chosen by the foot placement behavior.

Figure 5 shows the correspondence between clock cycles and the interpolated trajectory of the toe. There is one clock for each leg, each 180° out of phase, and each periodically wrapping as the gait advances (Figure 5a). One clock cycle corresponds to one step for its corresponding leg. The clock cycles drive most of the trajectory interpolation for the gait (Figure 5c), reliably sequencing controller events (as opposed to triggering based on intermittent events such as toe strike).

2) Stride Trajectory and Foot Placement: Footfalls are placed such that the robot's velocity gradually approaches the desired direction. The controller takes a directional influence from a human operator and attempts to move in that direction, but individual steps are not controlled by the operator.

Each step is calculated using a feed-forward model of toe placement based on the transverse velocity of the robot (removing the vertical component), as illustrated in Figure 6b. The initial calculation would ideally carry the robot along its current path if used repeatedly over a number of steps. The feed-forward model is augmented with PD control around the transverse velocity error in both x (forward) and y (right), which controls the acceleration and deceleration of the robot as new velocity commands are issued.

The continual stepping of the feet due to the clock cycle aids in controlling the velocity; no single footfall corrects the robot's velocity, and frequent stepping gives more opportunities to recover from disturbances. Disturbances and model errors will continually change the robot's velocity, so there is no reason to attempt to enforce deadbeat control; asymptotic control works very well in this case.

3) Touchdown Transitions: The virtual toe trajectory (the location of the toe for undeflected springs) is open-loop and continuous through stride, touchdown, and into stance. Mechanism compliance allows for a smooth transition and gradual change in contact forces between the toe and the ground, which impact at non-zero velocity.

Open-loop transitions are an important feature of the controller and are deliberately crafted to be independent of contact sensing, because sensing the exact moment of touchdown is deceptively difficult to achieve in practice[3]. In dynamic environments, it is not even useful to know a particular instant of touchdown because the foot may slide, break and make contact repeatedly (chatter), or sink into soft terrain.

One open-loop toe trajectory is continuous in the time before and after contact, but is designed to decompose into two distinct 'controllers' based on the *real-world* contact state. Stepping uses a ground-speed-matched trajectory where the toe vertically descends to the ground height at that point. This method does not care exactly when the foot contacts the ground, and the same vertical trajectory is followed after the foot makes contact. Before touchdown, this trajectory corresponds to a ground-speed-matching behavior, but after touchdown, the *same* trajectory continues to drive the foot into the ground, resulting in a nearly axial restorative force. This second behavior is the trivial stance controller for spring-mass robots: hold a constant leg length through stance, and balance the leg angle torques such that the contact force goes through the mass center of the robot.

4) Torso Balance: After toe contact is established, contact forces begin rising and expand the ability of the torso balance controller to apply hip torques against the ground. A friction cone approximation limits the balancing hip torques, preventing the toe from slipping on the ground as illustrated in Figure 6a. Torques are calculated for pitch and roll degrees of freedom using a feedback-linearization law to force the torso upright (Rezazadeh et al., 2015). The effect of this behavior is added to the nominal stance behavior of leg-length forces.

5) Energy Injection and Damping: A large part of the robustness of the controller comes from the addition of controlled damping. Motor trajectory following has PD gains tuned such that roughly half of the over-all leg compliance comes from the motor, and the other half comes from the passive springs. Having such soft gains makes the robot more compliant and also removes energy through damping in the motors and transmission.

Energy injection replenishes the system's mechanical energy after some is removed by damping, disturbances, or elevation changes. Through the first half of stance, the leg length is nominally constant, remaining a passive spring. In the second half of stance, the leg begins extending to drive the robot forward. The amount of extension is proportional to the desired transverse velocity, as visually indicated in Figure 6c.

The interplay of energy injection and damping has a stabilizing effect on the system. As a simple example, a

[3]switches bounce, force thresholds take time to reach, and either may be triggered accidentally.

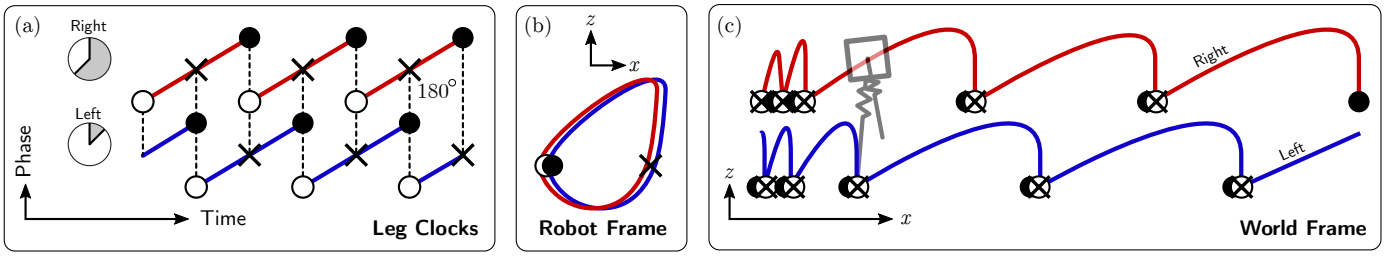

Fig. 5. (a) Two 180° out-of-phase clocks drive the leg motions. These clocks wrap from step to step and drive the periodic motions of the robot. (b) Toe trajectories as seen from the moving robot's frame. (c) Toe trajectories as they move through the world. Trajectories are shown for each leg (Right:Red, Left:Blue), and markings show the correspondence between clock and toe trajectories.

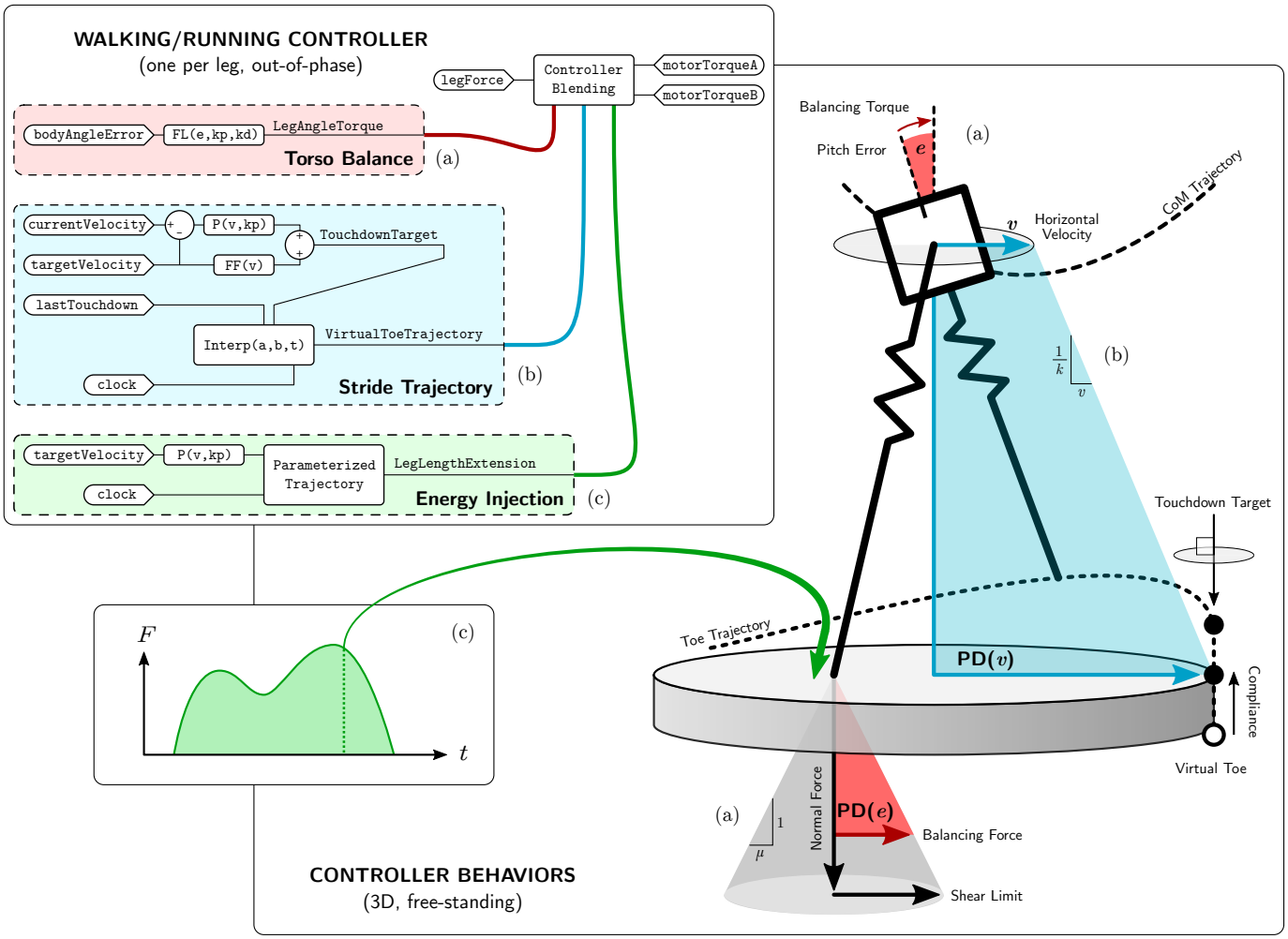

Fig. 6. High-level view of three main behaviors of the control algorithm. (a) Torso balance attempts to keep the torso upright, applying restoring torques at the hip based on a feedback-linearization (FL) control law. Because each leg has both stance and aerial phases, the balance controller must be blended in and out as the contact force changes. The resulting shear force on the ground is always limited to be within an approximate friction cone. (b) Each stride trajectory has a target touchdown location for the toe, where the toe will be ground-speed-matched and lowered toward the ground. This vertical descent continues even after the physical toe begins contact, and the virtual toe is driven deeper into the ground where the leg compliance can supply restoring forces. Vertical descent also improves the chances that a disturbance will affect the height of the contact only. The touchdown target location is a result of feed-forward (FF) processing of the current velocity adjusted by the difference between current and target velocities. (c) Energy injection is parameterized as extra leg extension in the second half of the stance phase. Stepping and energy injection are both driven by an internal clock cyclically progressing through the phase [0, 1).

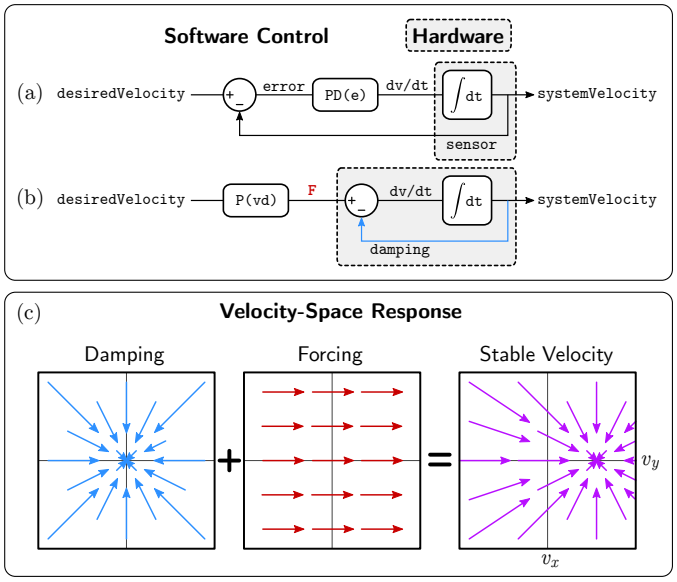

Fig. 7. A simple example of open-loop velocity control by balancing directional forcing against isotropic damping. (a) Feedback control of velocity requires an accurate measurement of the system velocity. (b) Feed-forward forces combine with damping in the world to close the feedback loop for velocity, with the added benefit that accurate sensing of the ground-truth velocity is no longer necessary, nor is accurate application of force in response to changes in velocity. (c) In velocity space, where the current velocity of a system is represented by a point in that space, forces represent the gradual change in position of those points. The force of damping always acts toward the origin. If an external force is applied, the equilibrium velocity shifts in the direction of that force.

vertical hopping robot can find an open-loop, stable hopping height by injecting a fixed amount of energy into each hop while leg damping removes energy proportional to touchdown velocity and stance duration; the energy injection will naturally balance the energy removal. Figure 7 shows how **physical damping can close the loop on velocity control**. Similarly for the ATRIAS robot, periodic forcing in the forward direction (through leg extension in the second-half of stance) finds a naturally-stable speed when balanced by the damping in the legs.

Figure 8 shows how the impulses generated by disturbances decay as a result of damping, and how **periodic forcing drives the robot forward without needing to directly sense and regulate velocity**.

III. Methods and Process

Having such an atypical design and control paradigm for a humanoid, ATRIAS required interactive tuning and gradual addition of behaviors to add capabilities to the controller. A high-fidelity SimMechanics model made it easy to continually tune and adjust controllers, with results that could be immediately used on the robot.

A. Tools

Having a quality software toolchain was vital for reaching the goal of a live show at the DRC. A combination of off-the-shelf software and hardware components were selected and assembled to form a control system which requires minimal maintenance effort. As an added benefit, the ATRIAS controller could be written as native MATLAB code. This toolchain allowed for rapid iteration of controllers and simple testing on the full-order robot.

A high-fidelity simulation of the ATRIAS biped allows for extremely efficient and worry-free testing of new control ideas (Martin et al., 2015). Modeled in SimMechanics and controlled through Simulink, the simulation is a good approximation of the behavior of the real robot, down to the same controller interface. A controller can be tuned using the simulation, then only require minor adjustment when implemented on the robot. The porting process is handled almost entirely by the software, requiring only a flag indicating whether the controller is running in the simulation or on the hardware.

Our final controller occupies a concise 880 lines of MATLAB code, not including the Simulink architecture. This does not include microcontroller or low-level safety code, only the final control function which maps robot state to motor commands.

Figure 9 shows the quality of the simulation, where the robot is kicked during a physical test and given the same impulse in simulation. Resulting robot trajectories are nearly identical, from the over-all torso path down to the motion and timing of the legs.

B. Development of Behaviors and Capabilities

We started with an intuitive, bare-bones controller for 2D push-assisted walking on a spherical boom. Adding a rear leg push-off behavior allowed the robot to walk on its own. This process continued, adding behaviors to the simulation, tuning, and applying them to the robot. Soon, we had a controller which could stably walk and run in 3D over rough and unstable terrain. There were several significant stages in developing this controller, starting with a basic controller and incrementally adding hand-coded behaviors.

1) State-based push-to-walk on flat ground (2D): The inaugural behavior is a stepping primitive with a fixed stride length, designed simply to put one foot in front of the other. This behavior is not automatic, so an operator must be present to push the robot forward from step to step. Stance leg and swing leg are determined by which physical leg is applying greater force to the ground, a parameter which typically switches when the hip is half way between footfalls. Forces in the leg-length and leg-angle are measured by sensing the deflection of the two series springs in each leg. To take the next step, the foot of the leading leg is brought to a point above the next target then lowered until it contacts the ground. The foot trajectory from previous midstride to next midstride is parameterized by the x-location of the hip between midstrides. After contact, the motors continue moving as if the foot was still in free space, causing the springs to deflect and apply a restorative force. Torso stabilization is achieved through P-D-controlled hip torques on the legs, scaled by the vertical ground force of each foot (i.e. scaled friction cone).

2) Self-regulated walking on flat ground: Adding a push-off behavior to the trailing leg allows the robot to propel itself

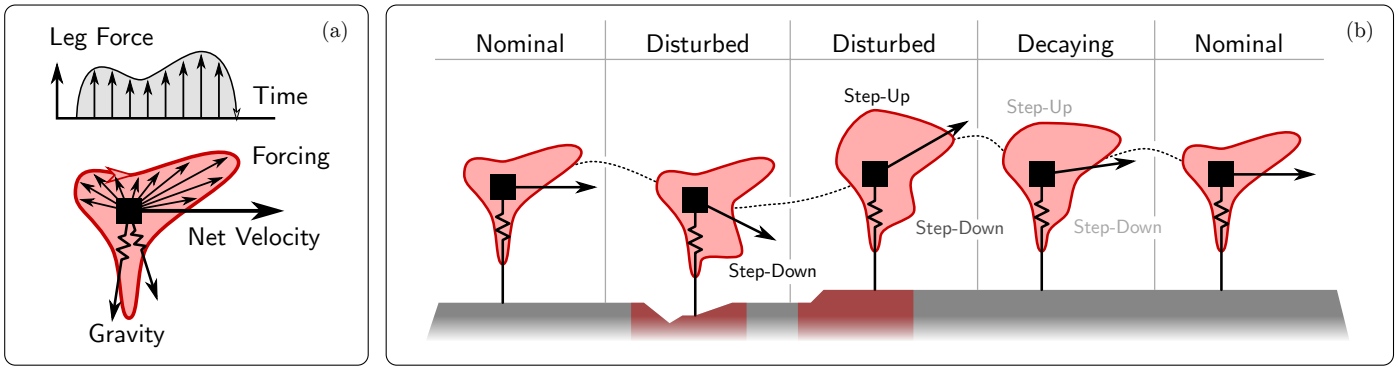

Fig. 8. The effect of physical damping on the net velocity of the robot. Envelopes around the mass center represent the history of directional impulses on the robot; impulses in the same direction sum, while impulses in different directions push out the envelope in those directions. The envelopes only record impulses from forces other than damping, which is represented by the gradual decay of the envelope. The average direction of the envelope gives the net velocity of the robot. The controller only needs to supply periodic forcing during locomotion, and damping will remove the effect of extraneous impulses due to disturbances. Damping also removes part of the effect of the periodic forcing, but that impulse is being continually injected, so it remains dominant. It is not necessary for the controller to sense and act on current velocity feedback, it must only supply feed-forward forcing in the desired direction.

Fig. 9. Example of the use of full-body simulation in the development of ATRIAS' control. (a) A film strip of the SimMechanics model of ATRIAS, with hardware controller, being simulated with a large horizontal impulse (aesthetically illustrated with an overlaid kicking human). (b) Using the same controller, the physical robot is kicked to test its disturbance rejection.

forward, adding back lost energy. Low proportional gains for the joint trajectories and high derivative gains damp energy out of the gait and stabilize the robot. The interaction between energy injection in the forward direction and energy removal by the joints leads to a stable forward walking speed.

3) Stepping in place (incorporating a clock-driven stepping cycle): The previous behaviors are not self-starting, so we add a clock-driven stepping cycle. This means the robot will always be in motion, even at zero forward velocity. It begins by stepping in place, trying to maintain a fixed horizontal position. Footfalls are selected to remove any extraneous momentum by shifting the horizontal position of the step proportionately with velocity error.

4) Speed changes, forward and reverse: With the stepping behavior implemented, we begin varying the forward velocity command from positive, to zero, to negative, and back. The robot begins by stepping in place at zero velocity, then slowly increases the forward speed to begin walking forward. The stride length is variable depending on the forward speed. The push off behavior is always in effect as a result of the clock-driven stepping cycle.

5) Lots of obstacles, stability testing: At this point, the controller is able to robustly walk over moderate step-ups, step-downs, loose terrain, and slippery terrain in 2D. It can also handle pushes and kicks which either accelerate or impede its forward progress.

6) Stepping in place (3D): The next big step in creating a controller for real-world locomotion is taking the robot off its support boom (the walking equivalent of removing the training wheels from a new cyclist's bike). Now, the robot must control its lateral velocity and torso roll in addition to forward velocity and pitch. We modify the clock-based stepping controller to account for these additional degrees of freedom rather than adding entirely new behaviors. The first test of this capability is simply stepping in place with a zero-velocity goal. At this point, we also make the strides fully dependent on the clock, removing any state-based feedback.

7) Robust stepping, obstacles, kicks, dodgeballs: Stability is the most important factor for real-world locomotion, so we spend time making sure the stepping controller can handle large velocity changes and changes in ground height and consistency. Our impulsive testing includes small pushes, a

dodgeball barrage, and heavy kicks. In separate tests, foam squares and wooden steps disrupt the flat-ground stepping cycle. The controller's behavior takes the extraneous velocities from these disturbances and removes them over several steps, settling into a zero-velocity stepping pattern.

8) Directed stepping: Just like stepping in place led to speed changes in 2D, the 3D stepping controller is given directional commands. A video game controller influences the velocity of the robot by 'suggesting' a direction of motion which the robot tries to satisfy. The speed change is not immediate, but the velocity asymptotically approaches the commanded speed and direction.

9) Robustness with obstacles: Another round of robustness testing for the directional walking controller, this time in 3D. More unstructured terrain is used, with foam pads, blocks, and plywood steps. At this point, we designed and built a lightweight mobile gantry that can be pushed around by a pair of researchers while a third drives the robot using the game controller.

10) Running over flat ground: Given enough space, the controller can pick up enough speed to find an aerial phase. Seeing as there is no ground contact in flight, we cannot judge the forward position of the robot through the stance leg. Instead, we judge forward position by integrating the last known forward velocity. Because forward velocity in flight is constant, and flight times are relatively small, this approach works well for maintaining ground-speed-matched toes.

IV. Locomotion Capabilities

We report ATRIAS' walking and running capabilities in terms of robustness (as measured by both terrain variation and external perturbations), speed, and energy economy. These abilities were assessed in a variety of experimental tests in the lead-up to the DARPA Robotics Challenge.

A. Robustness

ATRIAS' robustness to complex terrain was tested on a variety of surfaces, uneven structures, and inclines. Testing for nonrigid surfaces included grass, soft foam, and artificial field turf (snapshots in Figures 10(a), 10(e), 10(j)). Further, we tested spontaneous transitions between surfaces, to show robustness without any tuning of control parameters. Figure 10(b) shows a snapshot of ATRIAS transitioning between walking on grass and pavement, and Figure 10(e) between soft foam and particle board. This performance suggests that ATRIAS can walk stably without significant sensitivity to surface dynamics.

For our demonstration, we aimed to show locomotion on rough ground without any vision or prior planning. To create uneven ground in the laboratory, we tested walking on various arrangements of stacks of plywood. Figure 10(d) shows the robot walking quickly (1.8 m/s) on a randomly structured obstacle (maximum height 9.5 cm), coming to a controlled stop at the end of the structure. The most extreme laboratory obstacle tested was a 15-cm tall platform. In 11 consecutive tests, the robot successfully stepped onto this platform, walked a few elevated steps, and stepped off (shown in Figure 10(f)). Because the robot was unable to plan for the obstacle, some of the foot placements were not clean, including one test in which the robot landed on the obstacle on the point of its toe. The control algorithm was able to recover in spite of these unexpected contact modes and timings. Further, in an outdoor test, the robot was able to walk up and down a 15 degree slope (Figure 10(c)).

We also tested ATRIAS' response to unexpected disturbances, such as repeated dodgeball strikes (Figure 10(g)). To deliver a mucher larger test impulse to a human-sized robot, we gave the torso a series of firm kicks (Figure 10(h)). When stepping in place, the robot was able to recover from kicks imparting 60 kg m/s without falling[4] This impulse is the equivalent of instantaneously accelerating the robot to 1 m/s.

B. Speed

ATRIAS was able to match commanded speeds between zero and 2.5 m/s, and performed similarly well in both forward and reverse directions[5]. Figure 10(i) shows a snapshot of ATRIAS reaching its top speed of 2.5 m/s (9 kph) in an outdoor test on an asphalt path. After accelerating faster than 2.0 m/s, short aerial periods with no ground contact emerged, resulting in a transition to a running gait. This ability to transition between walking and running gaits was accomplished without switching between controller structures. Figure 10(j) shows a snapshot of ATRIAS after a transition to running during an outdoor test on artificial field turf, and Figure 10(k) shows corresponding ground-reaction forces measuring the length of aerial phases (an average flight time of 30 ms). This test also demonstrated the robot's ability to accelerate from rest to a run, and then execute a controlled stop.

C. Energy Economy

We measure ATRIAS energetic properties by two metrics: its operation time on a single battery charge and the Mechanical and Total Costs of Transport (COT). To test battery life, we commanded ATRIAS to step repeatedly in place until the battery pack was drained. The 48V, 10 A-hr battery pack was drained in approximately 30 minutes of operation.

Cost of Transport is a nondimensional measure of the energy required to move a unit distance. Mechanical Cost of Transport (MCoT) accounts for only the mechanical energy being delivered by the actuators. Total Cost of Transport (TCoT) includes not just the mechanical cost to locomote, but resistive losses in the electric motors and the on-board electronics overhead as well (including wireless communication and control computer). We calculate the TCoT and MCoT for a 1.6 m/s walking test of ATRIAS. On average, the TCoT is 1.3, as measured at the battery pack (current and voltage). The average MCoT is 0.96, as measured at the actuator outputs (torque and speed).

[4]The size of the impulse delivered was inferred from simulating impulse disturbances in the high-fidelity simulator.

[5]We noted that the robot had the ability to achieve slightly higher speeds in the direction depicted in Figure 10(i)

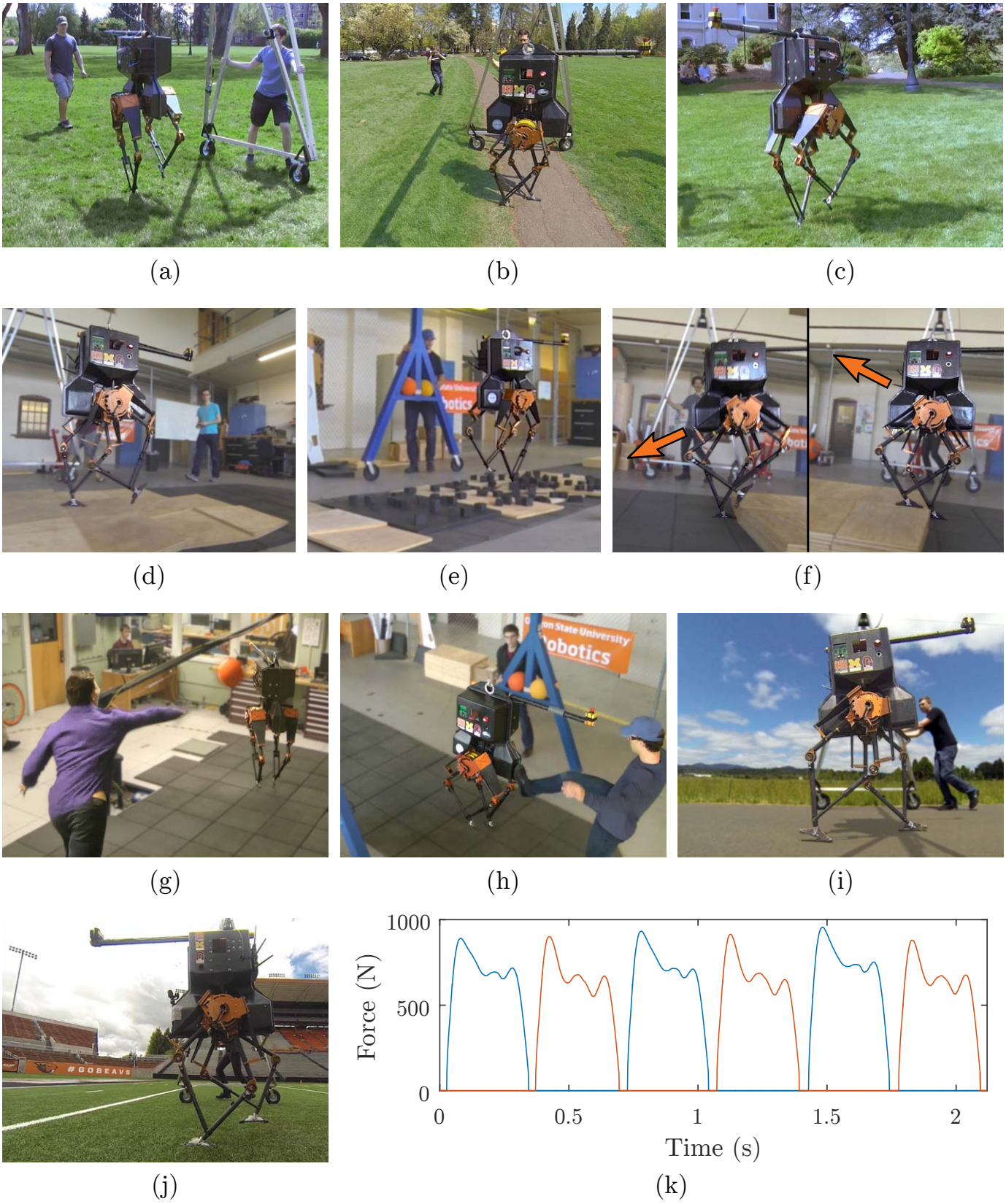

Fig. 10. Snapshots of various experiments with ATRIAS. The robot is shown (a) walking on grass, (b) transitioning from pavement to grass, and (c) walking up a 15-degree grassy slope. In-lab obstacles included (d) transitions between wooden boards and soft foam, (e) randomly structured boards, and (f) a 15-cm platform, all of which were negotiated blindly. External disturbances include (g) repeated dodgeball strikes and (h) large kicks. High speed tests include (i) a top speed of 2.5 m/s and (j) a smooth transition from rest to walking to running and back to rest on stadium turf. Plot (k) is shown for the vertical ground reaction forces for each leg, which gaps between indicating short periods of flight. Videos available online at (a-c) `https://youtu.be/dl7KUUVHC-M`, (d) `https://youtu.be/VBDysRlrfcY`, (e) `https://youtu.be/1CfHbBAv6vo`, (f) `https://youtu.be/dOoQTPqnLqI`, (g) `https://youtu.be/yYvrTc3-uVU`, (h) `https://youtu.be/K1m8fYsPMnY`, (i) `https://youtu.be/U4eBRPHYCdA`, and (j) `https://youtu.be/KeSkAPYAJc4`.

V. Demostration at the DARPA Robotics Challenge

Over the course of two days at the beginning of June 2015, ATRIAS had seven successful shows in front of live audiences in Pomona, California. Each show demonstrated walking over rough terrain, running on flat ground, kicks, and dodgeball impacts. Not once did ATRIAS crash or fall during these demonstrations. Four shows were performed beside our tent within the Expo area, and three shows were performed in front of the Fairplex Grandstands, where the main event was taking place.

VI. Lessons Learned

The ATRIAS biped pushes template matching to the extreme in its aim to embody the spring-loaded inverted pendulum (SLIP) model. It has carbon-fiber legs so light they are fairly fragile and require mechanical overload protection. Even at this end of the scale of passive dynamics, there are enough discrepancies between the reduced-order SLIP model and the robot to cause issues for model-based controllers. In the end, SLIP-inspired controllers were mixed with natural intuitions and tested in a high-fidelity simulation to achieve our results.

A. Practical Control Development

Design controllers based on reduced-order insights, but test with high-fidelity simulators. During early development, we would select touchdown leg angles for the full-order robot to try and affect a particular apex height and forward velocity for a SLIP model. A lot of effort was put into deadbeat controllers to move between apex states. An equal amount of effort was put into ground reaction force controllers and virtual-pivot-point controllers. As we found, these controllers were very sensitive to exact foot placement (cm variations would cause trouble) or to imprecise force vector control.

No robot will ever perfectly match a reduced-order model (at least not while matter still has mass), but it is easy for a robot to approximate simple spring-mass dynamics. The SLIP model is used extensively to inspire our controller, but that is where the relationship ends. We manually tune our controller in our high-fidelity simulation environment, finding natural frequency, stride-velocity proportionality, and other parameters which work for the full-order and heavily nonlinear system.

Exploit rapid iteration. The key to developing a working product, both hardware and software, is a quick design-test-evaluate cycle. Incremental testing allowed us to quickly test ideas, discover what works, and cut fruitless branches out of our search.

Allow for adjustable control parameters. Shifting model parameters are a fact of life in robotics. Not only does ATRIAS wear and age like any robot, it can also behave slightly differently with every test. Trimming controls like those for an RC airplane helped balance the robot on different terrain, with slightly different link lengths due to manufacturing, and different amounts of onboard weight. These tuning parameters are built into the controller and can be adjusted on the fly.

Be careful not to actively control any behavior which is actually a symptom of a more subtle control target. This difficulty occurs frequently in the field of bipedal locomotion: the most important feature of a gait appears to be the center-of-mass motion or ground-reaction forces, so many robots try to control exactly those. For highly underactuated and dynamic robots, controlling around a trajectory is extremely difficult; the control authority of the robot is limited and phase-dependent. Simply by choosing a different control target, like stride length, angular momentum, or vertical impulse, periodic CoM motions emerge naturally. Simple control targets generally require no pre-planning, and are reactive to changes in the environment, but they still excite the natural walking dynamics of the robot.

B. Moving Forward: Future Iterations

ATRIAS can walk and run at various speeds and over varied terrain, but has incredible difficulty standing still. The robot has a minuscule polygon of support, and active stabilization tests suggested just a tiny region of stability even in simulation[6]. While ATRIAS can hold position by stepping in place, this is not an energetically practical solution for idling. In future designs, having an ability to apply even limited stabilizing torques about the foot, while not impeding gait dynamics, would be helpful for stationary balancing, climbing stairs, and precise balancing between steps.

Turning is a major component of locomotion, but ATRIAS can only strafe. Animals are able to zig-zag and bank between obstacles and points of interest, and we want future robots to have the same ability. To do this, ATRIAS would need an extra actuator to control the long-axis rotation of the leg, applying yaw torques to the ground and turning the robot. Currently, the robot requires the human operator to manually steer via a carbon tube extending from its torso, and turning the robot breaks static friction between the feet and the ground.

Practical robots will need to be self-starting and self-parking. ATRIAS must be started from a hanging position, and the shut-down process effectively stops the robot in mid air and causes it to fall. Future iterations should be able to stand up on their own from a parked position and return to that position when shut down.

Escalating emergency states could gracefully handle small errors without a full emergency stop. Currently, there is only one e-stop case: shut down all motor drivers, crashing the robot. This case is triggered for everything from overheating motors and limit switch triggers to a dangerous controller failure. We disabled many of these safeties for the live shows at the DRC to prevent unnecessary halts.

Efficiency can continue being increased. ATRIAS uses Harmonic Drive gearheads for their small package, but they are extremely inefficient. In addition, an internal power loop where one motor acts as a brake saps valuable energy. Leg design must analyze the task force and speed requirements as they relate to the mechanism kinematics, minimizing the work lost to self-braking (Abate et al., 2015; Hubicki et al., 2015).

[6]Investigations into using LQR to locally stabilize a fixed point associated with standing yielded an impractically small basin of attraction.

The real world is a chaotic and dangerous place for robots, but machines with increased autonomy will need to be able to withstand and recover from crashes. ATRIAS requires a safety tether to prevent it from falling because it was designed to be a scientific demonstrator of spring-mass locomotion, not a durable field-ready product. Future robots should be sturdy enough to fall or crash into trees.

VII. Conclusion

The ATRIAS robot, with a combination of deliberately engineered passive dynamics and complementary control algorithms, was able to walk and run, without external power or support, in front of a live audience at the DARPA Robotics Challenge. In developing this live exposition, ATRIAS demonstrated 2.5 m/s running, variable speed control, and the ability to recover from large human kicks. Further, the robot was able to traverse varied surface dynamics and obstacles as high 15-cm without any planning or vision. To the best of our knowledge, this degree of terrain robustness has not been reported for a self-contained bipedal machine. What ultimately allowed for sufficiently fast progress was a commitment to rapid control iteration on hardware. However, by the nature of its highly compliant and underactuated design, every step along the way required ATRIAS to embrace its passive dynamics to keep moving forward.

Acknowledgment

The above work was funded by the following sources:

- Defense Advanced Research Projects Agency (DARPA), Maximum Mobility and Manipulation Program, Grant No. W31P4Q-13-C-0099 and W91CRB-11-1-0002
- Human Frontier Science Program (HFSP), Grant no. RGY0062/2010
- National Science Foundation (NSF), Grant no. CMMI-1100232

References

Andrew M Abate. Preserving the planar dynamics of a compliant bipedal robot with a yaw-stabilizing foot design, 2014.

Andy Abate, Ross L Hatton, and Jonathan Hurst. Passive-dynamic leg design for agile robots. In *Robotics and Automation (ICRA), 2015 IEEE International Conference on*, pages 4519–4524. IEEE, 2015.

Mojtaba Ahmadi and Martin Buehler. Controlled Passive Dynamic Running Experiments With the ARL-Monopod II. *IEEE Trans. on Robotics*, 22(5):974–986, 2006.

Pranav A. Bhounsule, Jason Cortell, Anoop Grewal, Bram Hendriksen, JG Daniël Karssen, Chandana Paul, and Andy Ruina. Low-bandwidth reflex-based control for lower power walking: 65 km on a single battery charge. *The International Journal of Robotics Research*, 33(10):1305–1321, 2014. doi: 10.1177/0278364914527485. URL `http://ijr.sagepub.com/content/33/10/1305.short`.

Reinhard Blickhan. The Spring Mass Model for Running and Hopping. *Journal of Biomechanics*, 22(11–12):1217–1227, 1989.

Reinhard Blickhan, Andre Seyfarth, Hartmut Geyer, Sten Grimmer, Heiko Wagner, and Michael Günther. Intelligence by mechanics. *Philosophical transactions. Series A, Mathematical, physical, and engineering sciences*, 365 (1850):199–220, jan 2007. ISSN 1364-503X. doi: 10.1098/rsta.2006.1911. URL `http://www.ncbi.nlm.nih.gov/pubmed/17148057`.

T. Boaventura, C. Semini, J. Buchli, M. Frigerio, M. Focchi, and D. G Caldwell. Dynamic torque control of a hydraulic quadruped robot. In *Robotics and Automation (ICRA), 2012 IEEE International Conference on*, pages 1889–1894, 2012. ISBN 9781467314053. URL `http://ieeexplore.ieee.org/xpls/abs{_}all.jsp?arnumber=6224628`.

B. G. Buss, A. Ramezani, K. Akbari Hamed, K. S. Griffin, B. A., Galloway, and J. W. Grizzle. Preliminary Walking Experiments with Underactuated 3D Bipedal Robot MARLO. In *Intelligent Robots and Systems (IROS 2014)*, pages 2529–2536. IEEE, 2014. URL `http://ieeexplore.ieee.org/xpls/abs{_}all.jsp?arnumber=6942907`.

S. H. Collins, A Ruina, R Tedrake, and M Wisse. Efficient bipedal robots based on passive-dynamic walkers. *Science*, 307(5712):1082–1085, 2005. doi: 10.1126/science.1107799.

Steven Hartley Collins and Andy Ruina. A Bipedal Walking Robot with Efficient and Human-Like Gait. In *IEEE Conference on Robotics and Automation*, number April, pages 1983 – 1988, 2005. ISBN 078038914X.

Monica A Daley and Andrew A. Biewener. Running over rough terrain reveals limb control for intrinsic stability. *Proceedings of the National Academy of Sciences of the United States of America*, 103(42):15681–15686, oct 2006. ISSN 0027-8424. doi: 10.1073/pnas.0601473103. URL `http://www.pubmedcentral.nih.gov/articlerender.fcgi?artid=1622881{&}tool=pmcentrez{&}rendertype=abstract`.

Tom Erez, Kendall Lowrey, Yuval Tassa, and Vikash Kumar. An integrated system for real-time Model Predictive Control of humanoid robots. In *IEEE/RAS International Conference on Humanoid Robots*, 2013. URL `http://homes.cs.washington.edu/{~}todorov/papers/ErezHumanoids13.pdf`.

M Ernst, H Geyer, and R Blickhan. Extension and customization of self-stability control in compliant legged systems. *Bioinspiration & biomimetics*, 7(4):046002, dec 2012. ISSN 1748-3190. doi: 10.1088/1748-3182/7/4/046002. URL `http://www.ncbi.nlm.nih.gov/pubmed/22791685`.

Siyuan Feng, Eric Whitman, X. Xinjilefu, and Christopher G. Atkeson. Optimization-based Full Body Control for the DARPA Robotics Challenge. *Journal of Field Robotics*, 32(2):293–312, mar 2015. ISSN 15564959. doi: 10.1002/rob.21559. URL `http://doi.wiley.com/10.1002/rob.21559`.

Robert J Full and Daniel E Koditschek. Templates and Anchors: Neuromechanical Hypotheses of Legged Locomotion on Land. *Journal of Experimental Biology*, 202

(23):3325–3332, dec 1999. ISSN 0022-0949. URL http://www.ncbi.nlm.nih.gov/pubmed/10562515.

Hartmut Geyer, Andrew Seyfarth, and Reinhard Blickhan. Compliant leg behaviour explains basic dynamics of walking and running. *Proc. R. Soc. Lond. B.*, 273(1603):2861–2867, nov 2006. ISSN 0962-8452. doi: 10.1098/rspb.2006.3637. URL http://www.pubmedcentral.nih.gov/articlerender.fcgi?artid=1664632{&}tool=pmcentrez{&}rendertype=abstract.

Ayonga Hereid, Shishir Kolathaya, Mikhail S. Jones, Johnathan Van Why, Jonathan W. Hurst, and Aaron D. Ames. Dynamic Multi-Domain Bipedal Walking with ATRIAS through SLIP based Human-Inspired Control. In *Hybrid Systems: Computation and Control*, 2014.

Christian Hubicki, Jesse Grimes, Mikhail Jones, Daniel Renjewski, Alexander Spröwitz, Andy Abate, and Jonathan Hurst. ATRIAS: Enabling Agile Bipedal Locomotion with a 3D-Capable Spring-Mass Robot Design. *In Revisions*, 2015.

Devin L Jindrich and Robert J Full. Dynamic stabilization of rapid hexapedal locomotion. *The Journal of experimental biology*, 205(Pt 18):2803–23, sep 2002. ISSN 0022-0949. URL http://www.ncbi.nlm.nih.gov/pubmed/12177146.

Matthew Johnson, Brandon Shrewsbury, Sylvain Bertrand, Tingfan Wu, Daniel Duran, Marshall Floyd, Peter Abeles, Douglas Stephen, Nathan Mertins, Alex Lesman, John Carff, William Rifenburgh, Pushyami Kaveti, Wessel Straatman, Jesper Smith, Maarten Griffioen, Brooke Layton, Tomas de Boer, Twan Koolen, Peter Neuhaus, and Jerry Pratt. Team IHMC's Lessons Learned from the DARPA Robotics Challenge Trials. *Journal of Field Robotics*, 32 (2):192–208, mar 2015. ISSN 15564959. doi: 10.1002/rob.21571. URL http://doi.wiley.com/10.1002/rob.21571.

S Kajita, F Kanehiro, K Kaneko, K Fujiwara, K Harada, K Yokoi, and H Hirukawa. Biped Walking Pattern Generation by using Preview Control of Zero-Moment Point. In *Robotics and Automation, 2003. Proceedings. ICRA '03. IEEE International Conference on*, pages 1620–1626, 2003.

Kenji Kaneko, Fumio Kanehiro, Mitsuharu Morisawa, Kanako Miura, Shin'ichiro Nakaoka, and Shuuji Kajita. Cybernetic human HRP-4C. In *2009 9th IEEE-RAS International Conference on Humanoid Robots*, pages 7–14. Ieee, dec 2009. ISBN 978-1-4244-4597-4. doi: 10.1109/ICHR.2009.5379537. URL http://ieeexplore.ieee.org/lpdocs/epic03/wrapper.htm?arnumber=5379537.

Stefan Kohlbrecher, Alberto Romay, Alexander Stumpf, Anant Gupta, Oskar von Stryk, Felipe Bacim, Doug A. Bowman, Alex Goins, Ravi Balasubramanian, and David C. Conner. Human-robot Teaming for Rescue Missions: Team ViGIR's Approach to the 2013 DARPA Robotics Challenge Trials. *Journal of Field Robotics*, 32(3):352–377, may 2015. ISSN 15564959. doi: 10.1002/rob.21558. URL http://doi.wiley.com/10.1002/rob.21558.

Scott Kuindersma, Robin Deits, Maurice Fallon Andr, Hongkai Dai, Frank Permenter, Koolen Pat, and Marion Russ. Optimization-based Locomotion Planning, Estimation, and Control Design for the Atlas Humanoid Robot. *Autonomous Robots*, 2015. doi: 10.1007/s10514-015-9479-3.

I. R. Manchester, U. Mettin, F. Iida, and R. Tedrake. Stable dynamic walking over uneven terrain. *The International Journal of Robotics Research*, 30(3):265–279, jan 2011. ISSN 0278-3649. doi: 10.1177/0278364910395339. URL http://ijr.sagepub.com/cgi/doi/10.1177/0278364910395339.

A. E. Martin, D. C. Post, and J. P. Schmiedeler. Design and experimental implementation of a hybrid zero dynamics-based controller for planar bipeds with curved feet. *The International Journal of Robotics Research*, 33 (7):988–1005, 2014. ISSN 0278-3649. doi: 10.1177/0278364914522141. URL http://ijr.sagepub.com/cgi/doi/10.1177/0278364914522141.

William C Martin, Albert Wu, and Hartmut Geyer. Robust spring mass model running for a physical bipedal robot. 2015.

T McGeer. Passive dynamic walking. *International Journal of Robotics Research*, 9(2):62–82, 1990.

Chet T Moritz and Claire T Farley. Passive dynamics change leg mechanics for an unexpected surface during human hopping. *Journal of applied physiology (Bethesda, Md. : 1985)*, 97(4):1313–22, oct 2004. ISSN 8750-7587. doi: 10.1152/japplphysiol.00393.2004. URL http://www.ncbi.nlm.nih.gov/pubmed/15169748.

Hae-won Park, Sangin Park, and Sangbae Kim. Variable-speed Quadrupedal Bounding Using Impulse Planning: Untethered High-speed 3D Running of MIT Cheetah 2. In *International Conference on Robotics and Automation*, pages 5163–5170, 2015. ISBN 9781479969227.

HW Park, Koushil Sreenath, Alireza Ramezani, and Jessy W. Grizzle. Switching control design for accommodating large step-down disturbances in bipedal robot walking. In *IEEE/RSJ International Conference on Robotics and Automation (ICRA)*, pages 45–50. Ieee, may 2012. ISBN 978-1-4673-1405-3. doi: 10.1109/ICRA.2012.6225056. URL http://ieeexplore.ieee.org/lpdocs/epic03/wrapper.htm?arnumber=6225056http://ieeexplore.ieee.org/xpls/abs{_}all.jsp?arnumber=6225056.

Ill W. Park, Jung Y. Kim, Jungho Lee, and Jun H. Oh. Online free walking trajectory generation for biped humanoid robot KHR-3(HUBO). *Proceedings - IEEE International Conference on Robotics and Automation*, 2006 (May):1231–1236, 2006. ISSN 10504729. doi: 10.1109/ROBOT.2006.1641877.

Rolf Pfeifer, Fumiya Iida, and Gabriel Gómez. Morphological computation for adaptive behavior and cognition. *International Congress Series*, 1291:22–29, jun 2006. ISSN 05315131. doi: 10.1016/j.ics.2005.12.080. URL http://linkinghub.elsevier.com/retrieve/pii/S0531513106001415.

Marc H. Raibert. *Legged robots that balance*, volume 29. MIT Press, Mass., 1986.

Siavash Rezazadeh, Christian M Hubicki, Mikhail Jones,

Andrew Peekema, Johnathan Van Why, Andy Abate, and Jonathan Hurst. Spring-mass Walking with ATRIAS in 3D: Robust Gait Control Spanning Zero to 4.3 KPH on a Heavily Underactuated Bipedal Robot. In *Proceedings of the ASME 2015 Dynamic Systems and Control Conference ASME/DSCC 2015*, 2015.

Y Sakagami, R Watanabe, C Aoyama, S Matsunaga, N Higaki, and K Fujimura. The intelligent ASIMO: system overview and integration. In *Intelligent Robots and Systems, 2002. IEEE/RSJ International Conference on*, pages 2478–2483, Lausanne, Switzerland, 2002.

J Schmitt and J Clark. Modeling posture-dependent leg actuation in sagittal plane locomotion. *Bioinspiration & Biomimetics*, 4(4):–, 2009.

William John Schwind. *Spring Loaded Inverted Pendulum Running: A Plant Model*. PhD thesis, University of Michigan, 1998.

Andre Seyfarth, Hartmut Geyer, and Hugh M Herr. Swing-leg retraction: a simple control model for stable running. *The Journal of Experimental Biology*, 206(15):2547–2555, aug 2003. ISSN 0022-0949. doi: 10.1242/jeb.00463. URL http://jeb.biologists.org/cgi/doi/10.1242/jeb.00463.

Mark Spong. Underactuated mechanical systems. In Bruno Siciliano and Kimon Valavanis, editors, *Control Problems in Robotics and Automation*, volume 230 of *Lecture Notes in Control and Information Sciences*, pages 135–150. Springer Berlin / Heidelberg, 1998. URL http://dx.doi.org/10.1007/BFb0015081.

M.˜W. Spong. Partial Feedback Linearization of Underactuated Mechanical Systems. In *IEEE/RSJ Intl. Conf. on Intelligent Robots and Systems*, pages 314–321, Munich, sep 1994.

K. Sreenath, H.-W. Park, I. Poulakakis, and J. Grizzle. Embedding active force control within the compliant hybrid zero dynamics to achieve stable, fast running on MABEL. *The International Journal of Robotics Research*, 32(3):324–345, mar 2013. ISSN 0278-3649. doi: 10.1177/0278364912473344. URL http://ijr.sagepub.com/cgi/doi/10.1177/0278364912473344.

Koushil Sreenath, Hae-won Park, Ioannis Poulakakis, and J W Grizzle. A Compliant Hybrid Zero Dynamics Controller for Stable, Efficient and Fast Bipedal Walking on MABEL. *International Journal of Robotics Research*, 30(9):1170–1193, 2011.

Hamid Reza Vejdani, Albert Wu, Hartmut Geyer, and Jonathan Hurst. Touch-down angle control for spring-mass walking. In *IEEE International Conference on Robotics and Automation (ICRA)*, pages 5101–5106, 2015. ISBN 9781479969227.

Miomir Vukobratovic and Branislav Borovac. Zero-moment point - thirty five years of its life. *International Journal of Humanoid Robotics*, 1(1):157–173, 2004.

PM Wensing and DE Orin. High-speed humanoid running through control with a 3D-SLIP model. *... and Systems (IROS), 2013 IEEE/RSJ ...*, pages 5134–5140, nov 2013. doi: 10.1109/IROS.2013.6697099. URL http://ieeexplore.ieee.org/lpdocs/epic03/wrapper.htm?arnumber=6697099http://ieeexplore.ieee.org/xpls/abs{_}all.jsp?arnumber=6697099.

E Westervelt, J W Grizzle, and D E Koditschek. Hybrid Zero Dynamics of Planar Biped Walkers. *IEEE Transactions on Automatic Control*, 48(1):42–56, jan 2003.

Seung-Joon Yi, Stephen G. McGill, Larry Vadakedathu, Qin He, Inyong Ha, Jeakweon Han, Hyunjong Song, Michael Rouleau, Byoung-Tak Zhang, Dennis Hong, Mark Yim, and Daniel D. Lee. Team THOR's Entry in the DARPA Robotics Challenge Trials 2013. *Journal of Field Robotics*, 32(3):315–335, may 2015. ISSN 15564959. doi: 10.1002/rob.21555. URL http://doi.wiley.com/10.1002/rob.21555.

Matt Zucker, Sungmoon Joo, Michael X. Grey, Christopher Rasmussen, Eric Huang, Michael Stilman, and Aaron Bobick. A General-purpose System for Teleoperation of the DRC-HUBO Humanoid Robot. *Journal of Field Robotics*, 32(3):336–351, may 2015. ISSN 15564959. doi: 10.1002/rob.21570. URL http://doi.wiley.com/10.1002/rob.21570.